A Quantum Mechanical and Statistical Mechanical Exploration of the Thermal Decarboxylation of Kemp's Other Acid (Benzisoxazole-3-carboxylic Acid). The Influence of Solvation on the Transition State Geometries and Kinetic Isotope Effects of a Reaction with an Awesome Solvent Effect

H. Zipse, G. Apaydin, and K. N. Houk*

Contribution from the Department of Chemistry and Biochemistry, University of California, Los Angeles, California 90095-1569

Received July 5, 1994[⊗]

Abstract: The decarboxylation of benzisoxazole-3-carboxylate has been investigated in detail by ab initio molecular orbital calculations. The effects of solvent on transition state geometries have been investigated by inclusion of one or two water molecules in the ab initio calculations. The decarboxylation and ring opening steps are found to be concerted. Kinetic isotope effects have been calculated for the carboxylate-^{13}C-labeled compound for various transition state geometries. Satisfactory agreement has been found between the experimental values for the reaction in water and ab initio HF/6-31G* calculated values for systems including four hydrogen bonds to the carboxylate group. The variations in free energies of solvation along the reaction path in five different solvents (water, methanol, chloroform, acetonitrile, tetrahydrofuran) have been calculated with Monte-Carlo free energy perturbation calculations. Solvent effects are generally overestimated, but the experimental trends have been reproduced for four of the five solvents. The effects of ion pairing have been tested by inclusion of a tetramethylguanidinium cation into the Monte-Carlo simulations for acetonitrile and tetrahydrofuran. With inclusion of ion pairing, the relative rates of THF and acetonitrile are reproduced much better, but solvent effects are underestimated relative to the reaction in water.

Introduction

The decarboxylation of benzisoxazole-3-carboxylic acids to form salicylonitriles has been investigated in extraordinary detail by Kemp *et al.*[1] The reaction involves the conversion of the conjugate base of benzisoxazole-3-carboxylic acid (**1**) to cyanophenoxide **3**, without formation of an intermediate (Scheme 1). The reaction rate is enormously sensitive to solvent polarity. There is a 10^8-fold increase in rate on changing the reaction medium from polar protic (H_2O) to polar aprotic (hexamethylphosphoramide). This has been explained by (1) stabilization of the carboxylate in protic media by hydrogen bonding, which raises the activation energy, and (2) stabilization of the charge-delocalized transition state, **2** through dispersion interactions with polarizable media. The second explanation rests on the assumption that the extended π-system is easier to polarize in the transition state than in the ground state. The importance of medium effects has been further defined through catalysis of the reaction by cationic and nonionic surfactants,[2] polymeric crown ethers,[3] and antibodies,[4] which speed up the reaction by factors of 4×10^2, 2×10^3, and 1×10^4, respectively, even in aqueous solution. Kinetic isotope effects for a $^{13}CO_2^-$ labeled structure have been measured by Hilvert *et al.* for the reactions in dioxane and water and for the antibody-catalyzed reaction in aqueous solution.[5] The KIEs of $k_{^{12}C}/k_{^{13}C} = 1.0434$, 1.0458, and 1.0484 measured for the reaction of 5-nitro-3-carboxybenzisoxazole in dioxane, water, and antibody-catalysis have been interpreted as proof for little variation in transition state geometry. The medium effect on the reaction has been further studied by multiparametric methods with Kamlet−Abraham−Taft methodology[6] and by the unified solvation model;[7] the solvent induced effects on the reaction rate were divided into the individual components. The analysis of these components has been used to interpret the mechanism of rate enhancement in the antibody binding site.

These data raise a variety of interesting questions. How does solvation alter the transition state structure? What is the relative degree of breaking of the C−CO_2 and N−O bonds in the transition state structure? Hilvert *et al.* concluded from their kinetic isotope studies that "changes in solvation do not seriously affect the transition-state structure"; can these geometrical effects be quantified? Furthermore, what information is obtained from isotope effects about immunoglobin catalyzed reactions? To answer these questions by theoretical methods, and to investigate the influence of hydration on rate and transition structures, the decarboxylation of benzisoxazole-3-carboxylate **1** (X = H) has been studied with ab initio methods. Furthermore, parameters

[⊗] Abstract published in *Advance ACS Abstracts*, May 15, 1995.

(1) (a) Casey, M. L.; Kemp, D. S.; Paul, K. G.; Cox, D. D. *J. Org. Chem.* **1973**, *38*, 2294. (b) Kemp, D. S.; Paul, K. G. *J. Am. Chem. Soc.* **1975**, *97*, 7305. (c) Kemp, D. S.; Cox, D. D.; Paul, K. G. *J. Am. Chem. Soc.* **1975**, *97*, 7312.

(2) (a) Bunton, C. A.; Minch, M. J.; Hidalgo, J.; Sepulveda, L. *J. Am. Chem. Soc.* **1973**, *95*, 3262. (b) Schmidtchen, F. P. *J. Chem. Soc., Perkin Trans. 2* **1989**, 135.

(3) (a) Shah, S. C.; Smid, J. *J. Am. Chem. Soc.* **1978**, *100*, 1426. (b) Shirai, M.; Smid, J. *J. Am. Chem. Soc.* **1980**, *102*, 2863.

(4) (a) Tarasow, T. M.; Lewis, C.; Hilvert, D. *J. Am. Chem. Soc.* **1994**, *116*, 7959. (b) Lewis, C.; Kreamer, T.; Robinson, S.; Hilvert, D. *Science* **1991**, *253*, 1019.

(5) Lewis, C.; Paneth, P.; O'Leary, M. H.; Hilvert, D. *J. Am. Chem. Soc.* **1993**, *115*, 1410.

(6) Grate, J. W.; McGill, R. A.; Hilvert, D. *J. Am. Chem. Soc.* **1993**, *115*, 8577.

(7) Ferris, D. C.; Drago, R. S. *J. Am. Chem. Soc.* **1994**, *116*, 7509.

(8) Frisch, M. J.; Head-Gordon, M.; Trucks, G. W.; Foresman, J. B.; Schlegel, H. B.; Raghavachari, K.; Robb, M. A.; Binkly, J. S.; Gonzalez, C.; DeFrees, D. J.; Fox, D. J.; Whiteside, R. A.; Seeger, R.; Melius, C. F.; Baker, J.; Martin, R. L.; Kahn, L. R.; Stewart, J. J. P.; Topiol, S.; Pople, J. A. *GAUSSIAN 90* and *GAUSSIAN 92*; Gaussian Inc.: Pittsburgh, PA, 1990.

0002-7863/95/1517-8608$09.00/0

Scheme 1

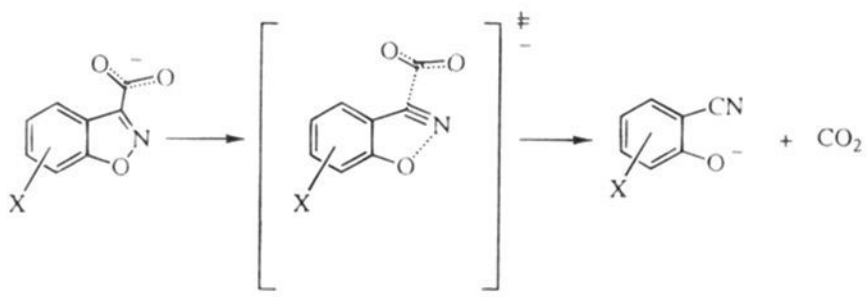

1 2 3 4

have been developed to calculate free energies of hydration along the reaction path by Monte-Carlo simulations.

Results

Ab initio molecular orbital calculations were carried out with Pople's GAUSSIAN 90 and GAUSSIAN 92 suites of programs.[8] Geometry optimizations have been carried out at the HF/3-21G level for the systems containing benzisoxazole-3-carboxylate with zero, one, or two water molecules. Some of the more interesting stationary points have been reoptimized at the HF/6-31G* level of theory. Vibrational frequencies and zero point energies (ZPE) were calculated for all stationary points. Energies were further evaluated with calculations of correlation energy at the second-order Møller−Plesset level (MP2/6-31G*) and, in part, with a larger basis set (MP2/6-31+G*). If not designated otherwise, relative energies in the text refer to the MP2/6-31G*//HF/3-21G+ΔZPE level. The frozen-core approximation has been used in all post Hartree−Fock calculations unless noted otherwise. Absolute energies for all stationary points are included in the supplementary material. For the calculation of solvation free energies, an ab initio reaction path has been calculated at the HF/3-21G level for the unsolvated system. Charges derived from Mulliken population analysis and by fitting the electrostatic potential using the CHELPG scheme[9] have been obtained by HF/6-31G* single point calculations on HF/3-21G geometries. Kinetic isotope effects have been calculated with QUIVER[10] at 293.15 K with a 20 cm^{-1} cutoff for low frequencies.

Monte-Carlo simulations have been performed with BOSS 3.1.[11] OPLS parameters for solvents were the standard Jorgensen parameters, while new OPLS parameters for reactant through transition state were developed from OPLS CHELPG charges. As a first step, changes in free energy of solvation (ΔG_{solv}) upon carboxylate group rotation were calculated for the ground state in four different solvents. Two different sets of Coulomb parameters were used in this part of the study to investigate how sensitive the results are to these parameters. The difference between ground state and transition state solvation has been calculated by perturbing the ground state structure in a stepwise fashion along the reaction path to the transition state. The use of different ground and transition state geometries has been studied to learn more about solvent-induced changes in the transition state.

Reaction without Solvation. The stationary points along the reaction path for decarboxylation of benzisoxazole-3-carboxylate were located by HF/3-21G and HF/6-31G* calculations. The rotation of the carboxylate group around the C−CO_2 bond was studied for both the ground state, **1**, and the transition state **2**, structures (Scheme 1, X = H). The lowest energy structures for **1** and **2** are found to be planar (Figure 1). The nonplanar conformation in which the carboxylate group is orthogonal to the π-system is a transition state for the rotation of the carboxylate group. The energy barriers for this rotation are 3.0 and 0.7 kcal/mol for **1** and **2**, respectively.

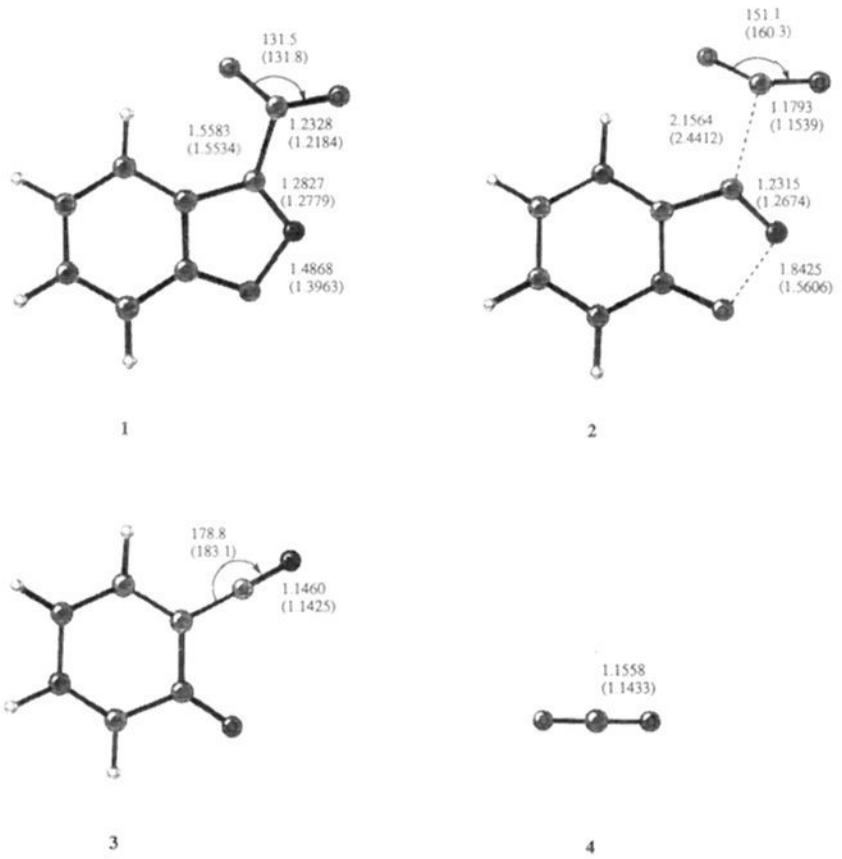

1 2 3 4

Figure 1. Geometries of benzisoxazole-3-carboxylate (**1**), transition structure for decarboxylation (**2**), and products (**3** and **4**). The bond lengths (Å) and angles (deg) are obtained from calculations with the 3-21G (6-31G*) basis set.

Optimizations with the HF/3-21G and 6-31G* basis sets give similar geometries for **1**. The most notable change can be seen in the ring N−O bond length which becomes shorter by more than 0.1 Å with the increase in the size of the basis set (Figure 1). Bond shortening is a consequence of inclusion of polarization functions and is a general phenomenon in molecules containing bonds between electronegative first-row elements.[12]

The structure of **2** differs from **1** most markedly in the N−O and C−CO_2 bond lengths and O−C−O bond angle (Figure 1). As the reaction proceeds, the N−O and C−CO_2 bonds stretch by 0.36 and 0.60 Å (3-21G) or 0.16 and 0.89 Å (6-31G*). The HF/6-31G* optimization results in a transition structure in which C−CO_2 bond breaking is more advanced and isoxazole ring opening is less advanced than in the HF/3-21G optimization. However, the result of both methods indicates that ring opening occurs simultaneously with decarboxylation. The alternative stepwise mechanism was also studied at the HF/3-21G level. The benzisoxazol-3-yl anion is not a stationary point on the potential energy surface. Instead, spontaneous ring opening occurs to give cyanophenoxide **3**.

Is it possible that, with better theoretical levels, a benzisoxazol-3-yl anion could be an intermediate on the potential energy surface? This question was investigated in more detail for the smaller model system *cis*-formaldoxime. The deprotonated form of *cis*-formaldoxime is an energy minimum at the HF/3-21G level, but not at 6-31G*, 6-31+G*, and MP2/6-31G* levels. In the last three cases, acetonitrile and hydroxide are obtained by optimization. A much clearer picture is obtained from the more complete model system, isoxazole. The cyclic anion is not an energy minimum at any of these levels. Instead, ring opening proceeds from the anion without any barrier to yield the acyclic *cis*-β-cyano enolate anion.

(9) Breneman, C. M.; Wiberg, K. B. *J. Comp. Chem.* **1990**, *11*, 431.
(10) Saunders, M.; Laidig, K. E.; Wolfsberg, M. *J. Am. Chem. Soc.* **1989**, *111*, 8989.
(11) (a) Jorgensen, W. L.; *BOSS*, Version 3.1; Yale University; New Haven, CT, 1991. (b) Jorgensen, W. L.; Gao, J. *J. Phys. Chem.* **1986**, *90*, 2174.
(12) Hehre, W. J.; Radom, L.; Schleyer, P. v. R.; Pople, J. A. Ab Initio Molecular Orbital Theory; Wiley: New York, 1985.

Table 1. Relative Energies (kcal/mol) of Stationary Points along the Reaction Coordinate in the Decarboxylation of Benzisoxazole-3-carboxylate

	E_a **3−1**	ΔE_{rxn} **5 + 6 − 1**
HF/3-21G//HF/3-21G	+19.3	−34.3
HF/3-21G//HF/3-21G+ΔZPE	+16.2	−31.0
HF/6-31G*//HF/3-21G	+24.8	−44.0
HF/6-31+G*//HF/3-21G	+26.4	−44.5
MP2/6-31G*//HF/3-21G	+16.7	−29.0
MP2/6-31+G*//HF/3-21G	+18.5	−27.3
MP2/6-31G*//HF/3-21G+ΔZPE	+13.6	−32.3
HF/6-31G*//HF/6-31G*	+23.4	−44.6
MP2/6-31G*//HF/6-31G*+ΔZPE	+19.1	−31.7

The activation barrier for decarboxylation of benzisoxazole-3-carboxylate in the gas phase is +13.6 and +19.1 kcal/mol for the 3-21G and 6-31G* potential surfaces, respectively. Single point calculations on the HF/3-21G optimized structures have been performed at the MP2/6-31+G* level as well (Table 1). Even though the MP2 energy of **1** is lowered by 35 kcal/mol on inclusion of diffuse basis functions, the relative energetics of **1**, **2**, and **3** + **4** are changed by less than 2 kcal/mol, the larger basis giving a higher activation barrier and a smaller exothermicity. Since very similar results are obtained with the 6-31G* and 6-31+G* basis sets, further single point calculations were performed with the 6-31G* basis sets only. Since activation barriers are known to be somewhat underestimated at the MP2/6-31G* level and overestimated at the RHF level, the gas phase activation barrier for decarboxylation can be estimated to be around +18 kcal/mol. The experimental enthalpy of activation in solution for X = H is $\Delta H^{\ddagger} = +32$ kcal/mol in water and $\Delta H^{\ddagger} = +25$ kcal/mol in acetonitrile.[1]

Major changes in the charge distribution must occur in the decarboxylation reaction. These are of special interest for solution simulations to follow. Partial atomic charges were calculated for the ground state, transition state, and the products, both with a Mulliken population analysis and by fitting the electrostatic potential to atomic point charges (Table 2). CHELPG gives a much smaller charge for the ring oxygen atom, and larger charges for the ring nitrogen for structures **1** and **2**. The carboxylate group in **1** is more negative with CHELPG than with Mulliken charges. In transition state **2**, these charges decrease. However, both methods predict that the overall charge of the carboxylate group on transformation from **1** to **3** decreases by almost the same factor. Both methods also give a very similar picture for the changes in the charge distribution of the aromatic π-system. About 60% of the decreased carboxylate charge appears as increased charge on the remaining four centers of the benzene ring.

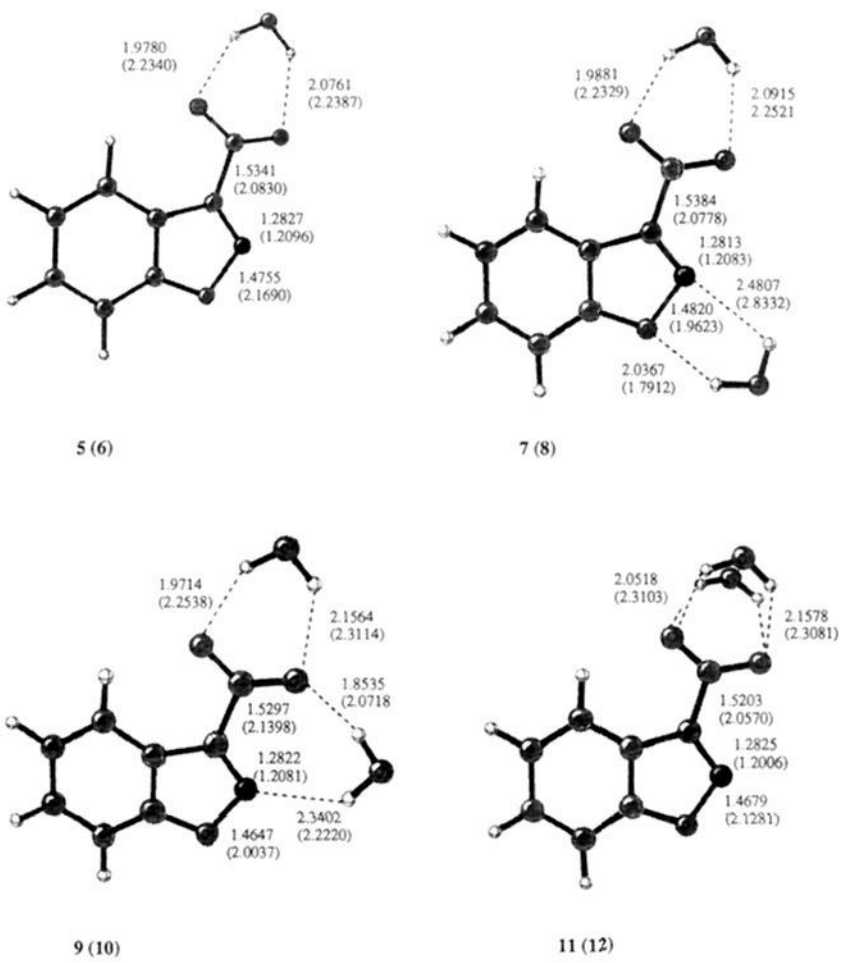

Figure 2. Various benzisoxazole-3-carboxylates hydrogen bonded to one or two water molecules. The numbers in parentheses are for the corresponding decarboxylation transition states.

Reaction in the Presence of Water Molecules. As a first step in the understanding of how solvent alters the activation energy to a large extent, and how this is reflected in the geometry of the transition state, we have studied the reaction including one or two complexing water molecules.

The carboxylate group is the strongest hydrogen bonding site in the reactant. Formate and acetate anions are most favorably complexed by one water molecule in a bifurcated, doubly hydrogen-bonded arrangement.[11b] One water molecule was therefore added to ground state, **1**, and transition state, **2**, in a bifurcated fashion (Figure 2, **5** and **6**, respectively). Ground state and transition state structures were also located for the decarboxylation in the presence of two water molecules arranged in three different ways (Figure 2). In all three structures, at least one water molecule is bound to the carboxylate group in

Table 2. Partial Charges for HF/3-21G Optimized Structures (HF/6-31G* Values Are Given in Parentheses Where Available)

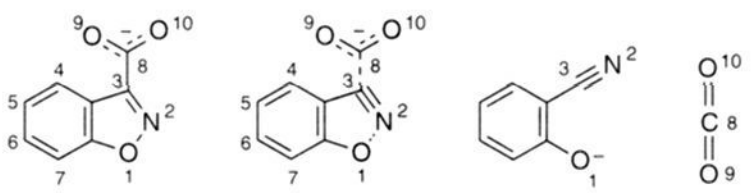

		center no.							
		1	2	3	8	9	10	CO_2	isoxazole
1	Mulliken	−0.619 (−0.574)	−0.190 (−0.172)	0.202 (0.177)	0.796 (0.777)	0.754 (−0.744)	−0.707 (−0.701)	−0.665 (−0.668)	−0.304 (−0.283)
	CHELPG	−0.306 (−0.255)	−0.378 (−0.391)	0.322 (0.285)	0.787 (0.816)	−0.790 (−0.800)	−0.762 (−0.777)	−0.765 (−0.761)	−0.007 (+0.013)
2	Mulliken	−0.732 (−0.648)	0.229 (−0.256)	0.097 (0.023)	0.877 (0.881)	−0.567 (−0.525)	−0.544 (−0.502)	−0.234 (−0.146)	−0.564 (−0.616)
	CHELPG	−0.559 (−0.415)	−0.293 (−0.343)	0.037 (−0.190)	0.838 (0.853)	−0.592 (−0.556)	−0.571 (−0.534)	−0.325 (−0.237)	−0.253 (−0.257)
3	Mulliken	−0.761	−0.559	0.294					
	CHELPG	0.775	−0.662	0.525					
4	Mulliken				0.902	−0.451			
	CHELPG				0.936	−0.468			
1−2	Mulliken							−0.431 (−0.522)	+0.260 (+0.363)
	CHELPG							−0.440 (−0.524)	+0.246 (+0.270)

Table 3. Differences [3-21G Values (in Å); 6-31G* Values (in Å) in Parentheses] between Geometries of Hydrated Species and Isolated Species and Transition States and Ground States in Different Model Systems

	$\Delta C-CO_2$	$\Delta N-O$	$\Delta C=N$
hydrated GS− unhydrated GS			
5−**1**	−0.02 (−0.01)	−0.01 (−0.01)	0.0 (0.0)
7−**1**	−0.02	−0.01	0.0
9−**1**	−0.03	−0.02	0.0
11−**1**	−0.04 (0.02)	−0.02 (−0.02)	0.0 (0.0)
hydrated TS− unhydrated TS			
6−**2**	−0.07 (−0.44)	+0.33 (+0.41)	−0.02 (−0.05)
8−**2**	−0.08	+0.12	−0.02
10−**2**	−0.02	+0.16	−0.02
12−**2**	−0.1 (−0.47)	+0.29 (+0.52)	−0.03 (−0.06)
TS−GS			
2−**1**	0.60 (0.89)	0.36 (0.16)	0.05 (0.01)
6−**5**	0.55 (0.46)	0.69 (0.58)	0.07 (0.06)
8−**7**	0.54	0.48	0.07
9−**10**	0.61	0.54	0.07
11−**12**	0.54 (0.44)	0.66 (0.70)	0.08 (0.07)

a bifurcated fashion. In **7** and **8**, the second water molecule complexes the nitrogen and oxygen atoms in the π-system. In **9** and **10**, the second water molecule is oriented such that bridging occurs between the isoxazole nitrogen and the *exo*-carboxylate oxygen atom. In **11** and **12**, the second water molecule is oriented in a bifurcated fashion, and four hydrogen bonds to the carboxylate group are formed.

The complexed ground and transition state structures were optimized at the HF/3-21G level. HF/6-31G* optimizations were also performed for the systems **5**(**6**) and **11**(**12**). Harmonic frequency calculations confirmed that these are the true minima and transition structures, respectively, except for structures **8** and **12**. Two imaginary frequencies of 532i and 16i cm^{-1} were found for **8** at the 3-21G level. The eigenvector of the larger imaginary frequency corresponds to the bond-breaking process, while the smaller frequency is associated with the out-of-plane bending of the water molecules. We have not investigated nonplanar structures, since the potential surface for such a motion is very flat. For structure **12**, three imaginary frequencies (566i, 56i, and 15i cm^{-1}) were obtained at the 6-31G* level. The smaller imaginary frequencies of 56i and 15i cm^{-1} correspond to rotation of the carboxylate group relative to the π-system as well as motion of the water molecules relative to the carboxylate group. Reoptimization of **11** and **12** without symmetry constrains leads to structures in which the carboxylate groups are twisted relative to the isoxazole π-system by about 65°. Since the potential surface for motions of the unbound water molecule proved to be very flat, full optimization to a stationary point was not attempted for either the ground or transition state.

Table 3 lists the changes in geometries induced by water molecules. The complexing of the ground state **1** by water molecules does not affect the structure significantly. Most notable changes, up to 0.04 Å, are observed on $C-CO_2$ bonds. The differences are even less at the 6-31G* level where available. The water molecules cause a more significant alteration to the transition structures. The 0.33 and 0.29 Å increases in the N−O bond length upon hydration are enormous changes. The relative degree of $C-CO_2$ and N−O bond breaking varies in different model systems. Decarboxylation is much less advanced, while the isoxazole ring opening is more advanced in the models **5**(**6**) and (**11**)**12**, where only the carboxylate is hydrogen bonded.

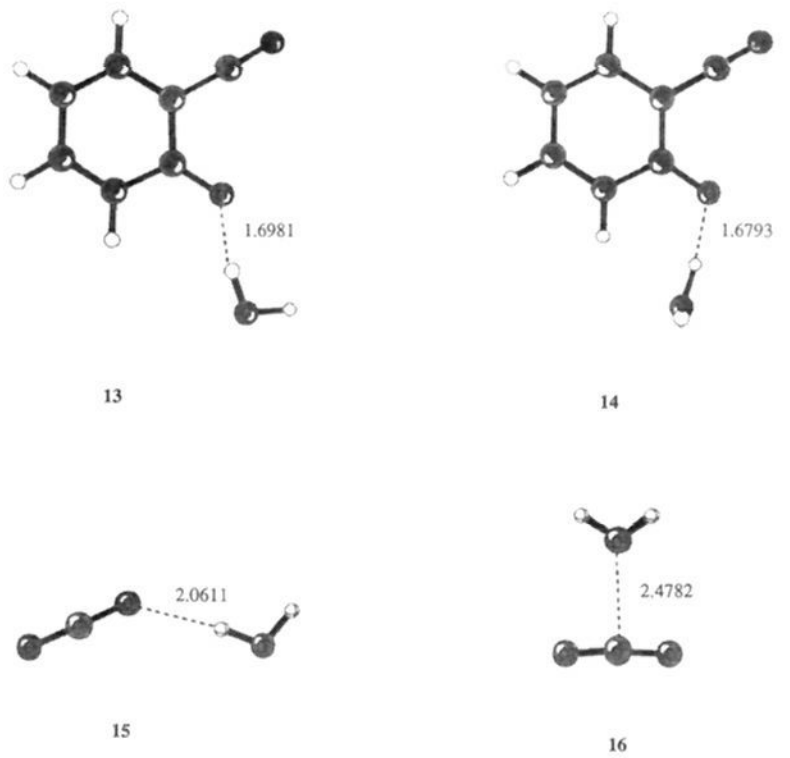

Figure 3. Structures of the decarboxylation products complexed by one water molecule at the HF/3-21G optimized level. Bond lengths are in angstroms and angles are in degrees.

Table 4. Relative Energies (kcal/mol) of Stationary Points along the Reaction Path in the Decarboxylation of Benzisoxazole-3-carboxylate in the Presence of One or Two Water Molecules

	E_c		
	GS	TS	E_a
5,6	−18.3	−9.0	+23.2
7,8	−26.1	−19.4	+20.3
9,10	−32.1	−20.0	+25.7
11,12	−30.8	−13.4	+31.0

The complexation energies (E_c) of benzisoxazole-3-carboxylate with water molecules in the ground and transition states are given in Table 4. The values of E_c are much lower for the transition states than for the ground states, because the concentrated charge in the ground state becomes dispersed in the transition states. Hydration increases the activation barrier (E_a) from +13.6 kcal/mol in the uncomplexed system to values shown in Table 4. With the model system **11**(**12**) the activation barrier rises to 31.0 kcal/mol, which represents the highest value of the systems considered. This value is fairly close to the experimental overall barrier of 32 kcal/mol in water.

The hydration of the reaction products has also been investigated (Figure 3). Planar, **13**, and nonplanar, **14**, conformations were studied for the cyanophenoxide. They are found to be virtually identical in energy; **13** is a transition state with one imaginary frequency for rotation of the water molecule (46i cm^{-1}), but the difference in zero-point energy compensates for the higher electronic energy. For the CO_2-H_2O complex, two conformations, **15** and **16**, have been found; **16** is slightly preferred over **15** without even forming a hydrogen bond. The hydration of anion **14** is, of course, much more favorable than nucleophilic complexation in **16** (−14.5 vs −1.7 kcal/mol). The decarboxylation reaction with one complexed water molecule is found to be exothermic by −28.6 kcal/mol, which is in good agreement with Kemp's estimate of approximately −30 kcal/mol in aqueous solution.

The Influence of Counterions. The decarboxylation rate can also be influenced by counterions of the benzisoxazole-3-carboxylate, especially in aprotic solvents. Rate measurements in these solvents by Kemp et al.[1] employed *N,N,N′,N′*-tetramethylguanidine (TMG) as a base, while triethylamine was used

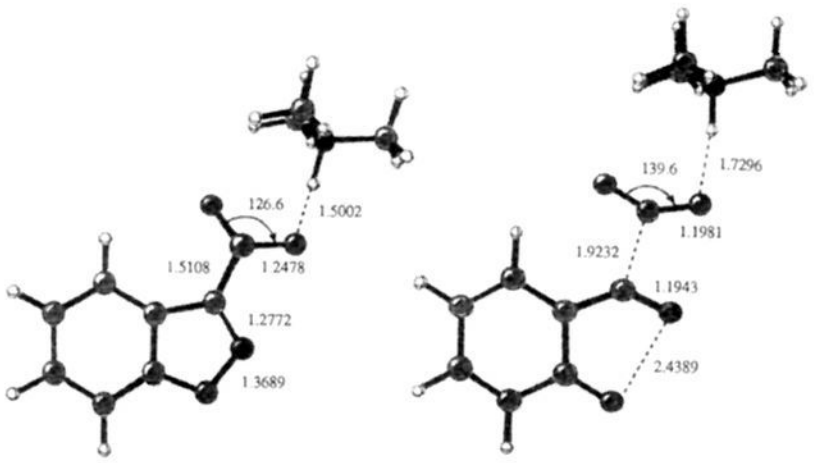

Figure 4. HF/6-31G* optimized ground and transition state structures in the decarboxylation reaction of benzisoxazole-3-carboxylate in the presence of trimethylammonium cation. Bond lengths are in angstroms and angles are in degrees.

in the kinetic isotope effect study by Hilvert *et al.*[5] Gas phase ion pairs are likely to be much tighter than solvated ion pairs, but the inclusion of the protonated base as a counterion in the gas phase ab initio calculations provides an upper limit for the activation barrier and for geometrical changes resulting from ion pairing. We added a trimethylammonium cation to the carboxylate group in the model system **1**(**2**). Reoptimization at the HF/6-31G* level gave ground and transition state structures, **17** and **18**, respectively (Figure 4). Ion pairing causes decreases in the C−CO_2 and N−O bond lengths in the ground state, 0.04 and 0.03 Å, respectively. However, the transition state structure, **18**, shows much larger geometrical deviations from transition structure **2**; there is a 0.52-Å decrease in the C−CO_2 bond length and a 0.88-Å increase in the N−O bond length. Even in this substantially asynchronous case, the reaction is still concerted. The dissociation energy of the ground state ion pair to ground state **1** and triethylammonium cation is +120 kcal/mol at the MP2/6-21G*//HF/6-31G*+ΔZPE level. The activation barrier is +62.4 kcal/mol at the same level. This exceeds the barrier found for the bishydrated system **11**(**12**) by 30.5 kcal/mol. The multiparameter analysis of the rate data for the decarboxylation of 6-nitro-3-carboxylbenzisoxazole in 20 different solvents by Grate *et al.* also shows that the reaction is slowed down significantly by ion pairing.[6] The result is expected because of the very high interaction energy which is lost as the decarboxylation proceeds. The result is not representative of a solution process, where the product ion pair between the cation and the phenoxide would also be highly stabilizing. However, it is revealing in terms of potential antibody binding by charged groups.

Kinetic Isotope Effects. Isotope effects have been used to provide experimental assessments of bond breaking in transition states. Hilvert *et al.*[5] have observed isotope effects of similar magnitude for the decarboxylation in dioxane, for water/buffer mixtures, and for the antibody-catalyzed reaction. The isotope effect provides information on changes in vibrational frequencies which are in turn a consequence of geometry and force constant changes. Because hydration causes a shift in transition state geometries, we calculated isotope effects to see how they change as the transition state geometries change. Vibrational harmonic frequencies calculated from HF/3-21G and HF/6-31G* force constants are usually too high by 10−20%. Consequently, scale factors between 0.9 and 0.8 are used to scale computed harmonic to experimentally observed frequencies. To determine scaling factors suitable for the system under investigation, harmonic frequencies were calculated for formic acid and carbon dioxide as model structures for the carboxylate group in its initial and final stages of the decarboxylation reaction. The calculated results were compared with relevant data from experimental gas phase spectra[13] of these molecules. Based on these results, scaling factors of 0.95 and 0.90 were used in this work for the HF/3-21G and HF/6-31G* vibrational frequencies, respectively.

Table 5. Calculated Kinetic Isotope Effects k_{12C}/k_{13C} and k_{16O}/k_{18O} and Activation Energies for Decarboxylation

reactant/ transition state	no. of H_2O	HF/3-21G		HF/6-31G*		
		k_{12C}/k_{13C}	E_a (kcal/mol)	k_{12C}/k_{13C}	k_{16O}/k_{18O}	E_a (kcal/mol)
1/2	0	1.0307	+13.6	1.0320	1.0151	+19.1
5/6	1	1.0370	+23.2	1.0425	1.0291	+23.8
7/8	2	1.0359	+20.3			
9/10	2	1.0371	+25.7			
11/12	2	1.0406	+31.0	1.0463	1.0337	+31.9
17/18	$TMGH^+$			1.0521		+62.4

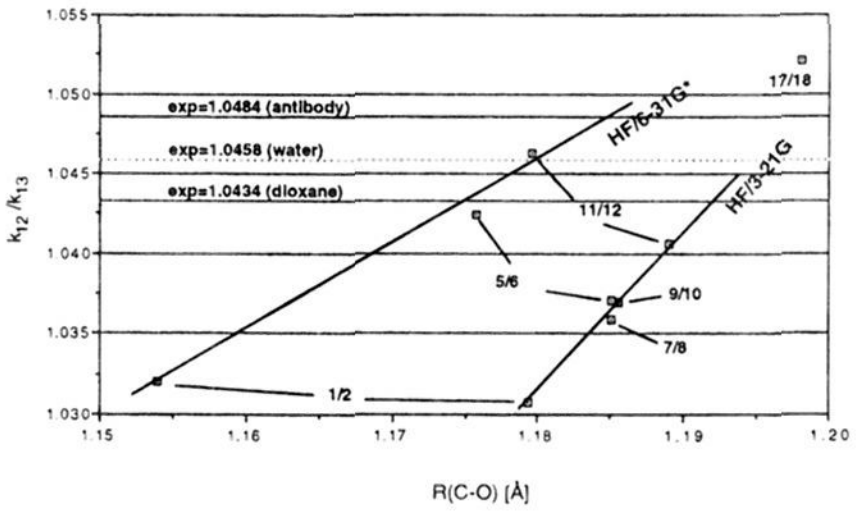

Figure 5. Kinetic isotope effects plotted versus the C−O bond length in the transition state.

Kinetic isotope effects were calculated for comparison to experimental isotope effects for decarboxylation. The k_{12}/k_{13} values obtained for the unhydrated and mono- and bishydrated systems using HF/3-21G and HF/6-31G* vibrational frequencies, where available, are collected in Table 5. In general, increasing KIEs are found at both levels as the number of hydrogen bonds formed between the water molecules and carboxylate group increases. The interpretation of the kinetic isotope effect data is quite complicated; in the present circumstance there are two types of bonds attached to the isotopically labeled carbon, one of which (C−CCO_2) is breaking and the other of which (C=O) is forming during the decarboxylation process. These two opposing effects should promote normal and inverse isotope effects, i.e. $k_{12}/k_{13} > 1$ and $k_{12}/k_{13} < 1$, respectively. Overall, however, normal isotope effects are observed experimentally and predicted for each of the model systems. A good correlation between the (exo) C−O bond length of the carboxylate group and the KIE is shown in Figure 5. The more advanced the C−C breaking and C−O forming, the smaller the predicted isotope effect. The maximum effect occurs with the ion pair, where there is a relatively small contraction of the CO bond length and significant CC breaking. When the degree of CC breaking increases, the CO contraction increases also, and the isotope effect decreases.

The smallest effect is calculated for the gas phase reaction. As waters are added, the isotope effect increases. Hydration of the carboxylate group influences both contributions to the isotope effect. The C−CO_2 bond breaking is less advanced upon hydration, leading to an increased normal isotope effect.

Inclusion of a second water molecule leads to a further increase in isotope effect when both water molecules are bound to the carboxylate group as in structures **11/12**. Complexation of the isoxazole moiety as in **7/8** and **9/10** hardly changes the

(13) Sadtler Standard Spectra Collection, 1980.

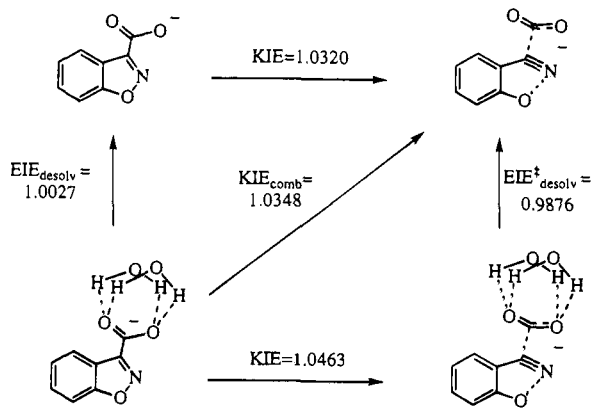

Figure 6. Kinetic and equilibrium isotope effects in the decarboxylation reaction of bishydrated and unhydrated benzisoxazole-3-carboxylate.

calculated KIE. At the HF/3-21G level, force constant changes are too small to reproduce the experimental KIE even in the system including four hydrogen bonds to the carboxylate group. The HF/6-31G* force constants lead to much closer agreement with experiment for the same system (Figure 5). At both levels, there is a strong correlation between the number of hydrogen bonds to the carboxylate group and the calculated KIE. This is also found for $^{16}O/^{18}O$-isotope effects calculated using the HF/6-31G* force constants by isotopic substitution of both carboxylate oxygen atoms (Table 5).

Primary carbon isotope effects have been reported by Hilvert et al. for the decarboxylation of the closely related 5-nitrobenzisoxazole-3-carboxylate with a ^{13}C-labeled carboxylate group.[5] The reaction shows KIEs of 1.0458 ± 0.0007, 1.0434 ± 0.0007, and 1.0484 ± 0.0009 in water, dioxane, and antibody catalysis in water, respectively. These values are marked with horizontal lines on the graph in Figure 5. The increase of KIE on changing the reaction medium from dioxane to water is in accord with the theoretical results discussed above, since complexation of the carboxylate group will be much stronger in a protic medium. The magnitude of the increase is much smaller than the calculated results for the change from gas phase to the bishydrated systems **11/12**. The KIE obtained for the antibody catalyzed reaction is still higher, suggesting an even stronger complexation of the carboxylate group. This conclusion runs contrary to the generally assumed mechanism of antibody catalysis, which is supposed to include binding of the substrate in an apolar pocket and desolvation of the carboxylate group.[5]

The computed results are not directly comparable to the experimental results because only models for aqueous solvation are available and because antibody-catalyzed reactions, like enzyme-catalyzed reactions, have isotope effects which are a composite of an equilibrium isotope effect for binding of the substrate and a kinetic effect for reaction of the bound substrate. Hilvert *et al.* assumed that the decarboxylation step in the antibody-catalyzed reaction has a KIE similar to the one found for the reaction in dioxane (1.0434). This implies there is an equilibrium isotope effect of EIE = 1.0048 for desolvation of the substrate. A thermodynamic cycle gives the corresponding isotope effect for desolvation of the transition state as EIE‡ = 1.0025.

We have calculated equilibrium isotope effects for desolvation of the bishydrated systems **11** and **12** using HF/6-31G* force constants (Figure 6) as a rough model for the experimental result. The EIE for desolvation of the ground state is about one-half of that calculated by Hilvert *et al.* A combined calculated isotope effect for desolvation of the bishydrated form and for decarboxylation of the unsolvated species is 1.0348. A similar value (1.0333) is obtained by combination of the KIE for the bishydrated system with the EIE$^{‡}_{desolv}$ = 0.9876 for desolvation of the transition state.

How can the large differences between the measured isotope effects for dioxane and the antibody-catalyzed reaction be reconciled with our calculations? As discussed in detail later, the decarboxylation may well involve ion pairs in dioxane solution. If only a small fraction of the gas phase ion pair effects persist in dioxane solution, a KIE significantly larger than that calculated for the uncoordinated carboxylate system **1/2** could result. The similarities of the isotope effects for the reactions in water and dioxane are then caused by complexation of the carboxylate group, by water molecules in one case and by ammonium cations in the other. The calculations on model systems indicate that strong carboxylate complexation causes the isotope effects in the range of 1.045−1.052, the range in which all the experimental isotope effects lie. These results suggest that the KIE measured for the antibody-catalyzed reaction reflects the binding of the carboxylate by strong proton donors in the binding pocket. Since anionic sulfonates were used as haptens, cationic groups are likely to be present in the binding pocket. This has also been suggested by Hilvert *et al.*[4]

Monte-Carlo Solution Simulations. The ab initio calculations show the important impact of hydration on the transition structure. Under experimental conditions, however, a much larger number of solvent molecules will be interacting with the solute simultaneously. This can be simulated with Monte Carlo (MC) or molecular dynamics (MD) solution simulations. The MC methods developed by Jorgensen *et al.* for organic systems allow the calculation of free energies of solvation for reactions.[11] Experimental data for the rate of decarboxylation of **1** are available for water, methanol, acetonitrile, and chloroform,[1] for which intermolecular potential parameters are also available for solution simulations. We have performed Monte-Carlo simulations of the decarboxylation in these four solvents.

Intermolecular Potential Functions. Standard OPLS potential function parameters have been used for the solvents as included in Version 3.1 of BOSS.[11a] The TIP4P water model was used. For the solute, HF/3-21G and, in part, HF/6-31G* optimized geometries were used. Lennard-Jones parameters for the solutes were taken from related compounds described in the literature.[14,15] Since the changes in charge distributions are expected to be the main factor for variations in solute−solvent interactions, the same set of Lennard-Jones parameters has been used for all solutes. Coulomb parameters were first derived by a HF/6-31G* Mulliken population analysis on the HF/3-21G geometries. Interaction energies for monohydrations were calculated with these parameters and were compared with ab initio values. Intermolecular geometrical parameters between **1** in its HF/3-21G geometry and one TIP4P water molecule were optimized at the HF/3-21G level. Single point calculations were then performed on the optimized complexes at the HF/6-31G* level. The energies obtained from the supermolecule calculation were then compared with HF/6-31G* energies of the separate components at identical geometries. Complexation energies for the carboxylate group in **1** are between 14 and 17 kcal/mol. The bifurcated orientation as in **5** is found to be the most stable, with ΔE = −16.7 kcal/mol. This is comparable to results obtained in hydrations of formate and acetate anions.[11b] This value is also very close to the complexation energies calculated by HF/6-31G* or MP2/6-31G* single points in the fully HF/3-21G or HF/6-31G* optimized structure, **5**. The use of rigid

(14) Jorgensen, W. L.; Severance, D. L. *J. Am. Chem. Soc.* **1990**, *112*, 4768.

(15) Jorgensen, W. L.; Chandrasekhar, J.; Madura, J. D.; Impey, R. W.; Klein, M. L. *J. Chem. Phys.* **1983**, *79*, 926.

TIP4P water and benzisoxazole-3-carboxylate geometries introduces no major error in the calculation of monohydration energies.

Monohydration of the isoxazole moiety yields interaction energies between 6 and 8 kcal/mol. Edge-on complexation of the benzene ring gives only a small interaction energy of about 1.7 kcal/mol. The hydration energies of the carboxylate are calculated to be slightly too small using Mulliken charges, but hydration energies for the isoxazole ring are much too high. The charge of the isoxazole oxygen seemed to be the major source of the problem. A strong decrease in oxygen charge, together with slight increases of the carboxylate oxygens charges and decreases in the positive charges of centers in the benzene ring, gave a much better fit with the ab initio values. This parameter set with "adjusted" HF/6-31G* Mulliken charges was consequently used in the liquid simulations of ground state rotation in all four solvents. As a last step, the HF/6-31G*// HF/3-21G electrostatic potential was fit to point charges with CHELPG. Interaction energies calculated with these charges are slightly better than those calculated with the adjusted Mulliken charges. The use of CHELPG charges avoids the very time consuming monohydration study. CHELPG charges have therefore been used in the liquid simulation of carboxylate group rotation in the ground state in water and in the solution simulations of carboxylate group rotation in the transition state as well as in the reaction path study in all four solvents.

Solution Simulation of the Ground State. Monte-Carlo simulations were first carried out for the ground state **1** to calculate the changes in free energy of solvation ΔG_{solv} during carboxylate group rotation. HF/3-21G optimized geometries were used for this study. The solute−solvent cutoffs for interaction energies were set at 11.0 Å in all solvents. The solvent−solvent energy cutoff was at 8.5 Å in water and at 10.0 Å in all other solvents. The simulations included 500 TIP4P water, 261 methanol, 188 acetonitrile, and 125 chloroform solvent molecules, respectively. The initial solvent geometries were taken from solvent boxes equilibrated at 25 °C. The NPT ensemble was used at 30 °C and 1 atm in each case. The structure of **1** was perturbed to the rotational transition state in ten steps. Double wide sampling was used such that the reference configuration was perturbed by ca. 5% in each direction. After 1.2M configurations of equilibration, actual sampling involved 4M configurations.

The changes in free energy of solvation (ΔG_{solv}) on carboxylate group rotation show that the rotational transition state is solvated better than planar conformation **1** in all four solvents. The relative stabilization of the rotational transition state is H_2O > MeOH > MeCN > $CHCl_3$. The gas phase ab initio energy of the rotational transition state is 3.0 kcal/mol higher than that of **1**. Water reduces this to about zero, and the rotational barrier is also lowered by other polar solvents. Nonplanar conformations, although not more stable than **1**, are likely to be more populated in protic solvents than in nonpolar solvents or the gas phase.

The use of CHELPG instead of adjusted Mulliken charges has only minor effects on the changes in ΔG_{solv}. This has been investigated for water as solvent. Overall, very similar results are obtained with both sets of charges. CHELPG charges give somewhat higher (more negative) free energies of solvation. At rotational angles of around 80−90°, larger differences can be observed. The considerably better solvation of the rotational transition state as compared to **1** can be attributed to better steric accessibility of the carboxylate oxygen atoms in the orthogonal structure. From integration of the radial distribution functions for the carboxylate oxygen atoms, the number of hydrogen bonds in **1** and the rotational transition state is found to be 5.25 and 5.88, respectively. The distribution of solute−solvent interaction energies shows a smaller number of strong hydrogen bonds (between −11.0 and −14.0 kcal/mol) for **1** as compared to the rotational transition state structure. The partial charges on the carboxylate oxygen atoms seems to be more important than the overall charge of the carboxylate group, which is more negative in **1** (−0.77e) as compared to the orthogonal structure (−0.70e).

Changes in Free Energy of Solvation along the Reaction Path. The changes in free energy of solvation have first been calculated for the HF/3-21G reaction path. The ab initio reaction path was followed up to C−CO_2 bond distances of 2.44 Å in 17 steps. The same Lennard-Jones parameters have been used for all intermediate geometries of the solute. The Coulomb parameters have been obtained for each step by fitting the HF/6-31G* electrostatic potential with the CHELPG method. The change in free energy of solvation was calculated for each step by perturbing one frame to the next one in one run with double wide sampling. After 1M iterations for equilibration, averaging was performed for 4M iterations for each step. In addition to the four solvents used in the first part, we also studied tetrahydrofuran, employing a box of 125 THF molecules.

The resulting changes in ΔG_{solv} are shown in Figure 7. The free energy of solvation is highest (most negative) for ground state **1** at R(C−CO_2) = 1.558 Å. Following the reaction path toward the gas phase transition state, the free energy of solvation decreases in all four solvents. The ΔG_{solv} values are therefore positive for all points along the reaction path. The least solvation occurs at R(C−CO_2) values between 2.1 and 2.2 Å in all four solvents, which is fairly close to the location of the gas phase transition state at 2.16 Å. The maximum in the ΔG_{solv} curves is located at the smallest R(C−CO_2) values for water, followed by the one for methanol and finally those for acetonitrile, THF, and chloroform. After these maxima, the ΔG_{solv} curve falls off again to values around 2.4 Å, where the free energy of solvation remains constant for protic solvents. The solvation does not change the location of maxima or minima on the potential energy surface but rather attenuates the energy difference between stationary points on this surface. This is well in line with Kemp's prediction of little variation in the structure of the transition states, which was based on the observation of only small solvent-induced variations in Hammett ϱ's obtained from reactions of substituted systems. For a more quantitative discussion, the differences in free energy of solvation between the ground state and the transition state have been collected in Table 6 together with experimentally determined relative rates at 30 °C. The differences in free energy of activation obtained from these data can be compared with the differences in free energy of solvation calculated with the MC method. It can be seen that the current model overestimates the solvent effects for the reaction. Rate data for the decarboxylation of **1** in chloroform and THF are not available. Decarboxylations of the 6-nitro-substituted derivative have been investigated in a large range of solvents, and rates in THF and chloroform are available.[1] The decarboxylation rates for these two substrates show a very good correlation:

$$k_{(NO_2)} = 1.326 + 1.037k_{(H)}; \quad R^2 = 0.993$$

From this correlation, rate data can be extrapolated for the reaction of **1** in THF and chloroform. A surprisingly slow rate is obtained for the reaction in chloroform, which has been explained by Kemp *et al.* by invoking the hydrogen bonding properties of this solvent. The MC simulation in this solvent

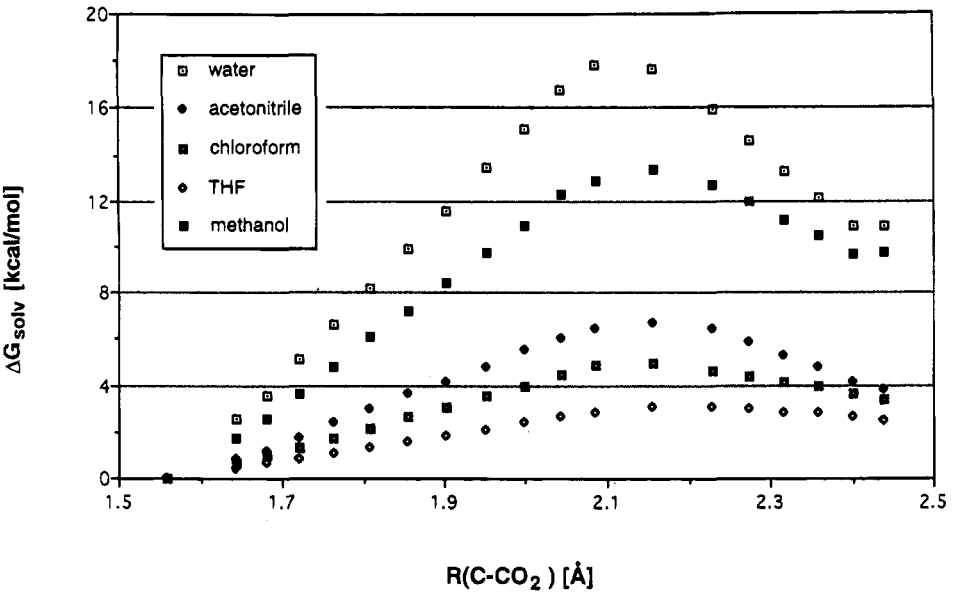

Figure 7. Changes in free energy of solvation along the HF/3-21G reaction path for the decarboxylation of benzisoxazole-3-carboxylate **1**.

Table 6. Comparison of Measured and Calculated Variations in Free Energy of Solvation for the Decarboxylation Reaction in Various Solvent (Relative Free Energies of Solvation Are Given in Parentheses)

			BOSS $\Delta\Delta G_{SOLV}$ (kcal/mol)				
solvent	k_{REL} (s^{-1})	$\Delta\Delta G^{\ddagger}$ (s^{-1})	HF/3-21G	HF/6-31G*	HF/6-31G* + $2H_2O$	HF/6-31G* + $2H_2O$ (H_2O only)	HF/3-21G + counterion
water	1	0	0.0	0.0	0.0	0.0	0.0
methanol	16.0	−1.67	−4.51 ± 0.23	−5.22 ± 0.28	−4.58 ± 0.26	−4.54	
chloroform[a]	54.3	−2.41	−12.98 ± 0.18	−14.71 ± 0.20	−13.78 ± 0.21	−14.03	
acetonitrile	113240	−7.01	−11.09 ± 0.20	−11.22 ± 0.26	−13.06 ± 0.24	−10.54	−4.67
THF[a]	185223	−7.31	−14.88	−16.92	−16.11	−16.24	−6.17

[a] Values extrapolated from correlation of benzisoxazole and 6-nitrobenzisoxazole-3-carboxylate rate data.

shows, however, very small variations in ΔG_{solv} along the reaction path.

To investigate if different transition state models would give better agreement between experiment and simulation, the HF/3-21G ground and transition state structures have been perturbed to the stationary points found at the HF/6-31G* level and to the structures found at the HF/6-31G* level including two water molecules (structures **11** and **12**). Coulomb parameters have been obtained again by fitting the HF/6-31G* electrostatic potential, excluding the two water molecules of the **11/12** system. Values obtained by using either the HF/6-31G* or the HF/6-31G* + $2H_2O$ stationary points show rather less correspondence with the differences in rate data (Table 4, BOSS $\Delta\Delta G_{solv}$, columns 2 and 3 of BOSS results). Since the MC simulations were performed with identical Lennard-Jones potentials, the different results must be attributed to variations in Coulomb parameters and transition state structures. Figure 8 gives an overview over the different structural situations at the stationary points of the three theoretical models in the form of a More-O'Ferrall–Jencks diagram.[16] The heavy open boxes mark points along the HF/3-21G reaction path. The ground state is located at the lower left corner. The additional boxes mark the ground states and transition states on the HF/6-31G*, HF/6-3/G* + $1H_2O$, and HF/6-31G* + $2H_2O$ potential surfaces. While the three ground states are close to each other, the transition states are quite different. The HF/6-31G* transition state is located far to the top left with a much larger C−CO_2 and a much shorter N−O bond length. Upon inclusion of one or two water molecules, the transition state shifts far to the right with a much shorter C−CO_2 and a much longer N−O bond length. The four transition structures included in Figure 8 appear to lie on a curve more or less orthogonal to the curve describing the HF/3-21G reaction path, forming a "transition ridge" that separates the reactant from the product potential energy valley. Solvation therefore seems to have a larger influence on the location of this ridge.

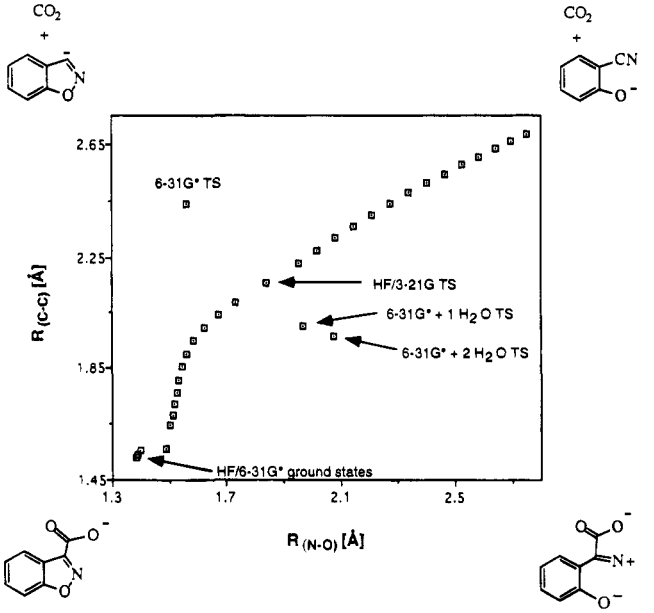

Figure 8. Changes in C−C and N−O bond lengths along the HF/3-21G reaction path including the location of stationary points on the HF/6-31G*, HF/6-31G*+$1H_2O$, and HF/6-31G*+$2H_2O$ potential energy surface.

(16) More O'Ferrall, R. A. *J. Chem. Soc. B* **1970**, 274.

The possibility that there are different transition structures in different solvents was also explored by assuming the hydrated HF/6-31G* transition structures only for water as a solvent and the uncomplexed HF/6-31G* structure for all other solvents. The resulting activation energies (Table 4, BOSS $\Delta\Delta G_{solv}$, column 4) are very similar to the HF/6-31G* values and also show an overestimation of solvent effects. The calculated free energy of hydration difference between ground and transition states **11/12** of +19.7 kcal/mol can also be combined with Gao's estimated gas phase free energy of activation ΔG^{298} of 15.4 kcal/mol to yield an overall free energy of activation $\Delta G^{\ddagger}(298)$ = 35.1 kcal/mol.[17] This is significantly higher than the value of 26.1 kcal/mol estimated by Gao, which is in good agreement with the experimental value of +26.3 kcal/mol. From both the overestimated $\Delta G^{\ddagger}(298)$ and relative free energies of activation in different solvents, it appears that the method of deriving monopole charges by fitting the HF/6-31G* electrostatic potential may lead to an overestimation of intermolecular Coulomb interactions for these charged species. Alternatively, it is possible that ion pairing must be included in the simulations, as described below.

Solution Simulation of Rotation in the Transition State. As a final step, a solution simulation was performed for the variation of ΔG_{solv} upon carboxylate group rotation in transition state **2**. Structure **2** was perturbed to the transition state in the reaction coordinate in ten steps. HF/3-21G geometries and HF/6-31G* CHELPG charges have been employed. Double wide sampling was used in each step with the reference configuration located halfway between the two structures. Each step included equilibration for 1M configurations and averaging of 500 water molecules only. The highest free energy of solvation is located at rotational angles around 70−75°. The ΔG_{solv} is 2 kcal/mol higher in this region than for the planar conformation. Carboxylate group rotation is likely to stabilize the transition state by approximately 1 kcal/mol. Since this stabilization is only available in water or other strongly hydrogen bonding solvents, it also changes the differences in free energies of solvation between different solvents by the same amount and will slightly reduce the overestimation of solvent effects.

The Effects of Ion Pairing in Solution. The possibility of ion pairing effects has already been discussed here in the context of the kinetic isotope effects as well as earlier in the literature.[1,3] The dramatic influence of an ammonium counterion on the transition state geometry and reaction energetics has already been demonstrated by ab initio calculations for the gas phase. This picture, however, is likely to be dramatically altered by solvent. In their kinetic studies, Kemp *et al.* frequently used *N,N,N′,N′*-tetramethylguanidine (TMG) as base to form the reactive carboxylate anion from the acid.[1] In most of the solvents investigated, the TMG cation was present as the counterion. How would the presence of this counterion affect the reaction energetics? We have extended our OPLS models for the HF/3-21G ground and transition state by inclusion of the TMG cation. The TMG geometry was optimized at the HF/6-31G* level using C_2 symmetry. The resulting structure proved to be a minimum after calculation of the vibrational frequencies. No other energy minimum could be found in a conformational search, even without symmetry constrains. Lennard-Jones parameters were chosen from the OPLS parameter set for guanidine and alkylamines.[11b,15] ESP charges were calculated as before by fitting the HF/6-31G* electrostatic potential. The benzisoxazole-3-carboxylate and TMG ions were initially positioned 2.8 Å apart and placed in boxes of 393 CH_3CN or 396 THF molecules. The reaction coordinate was defined

(17) Gao, J. *J. Am. Chem. Soc.* **1995**, *117*, 8600−8607.

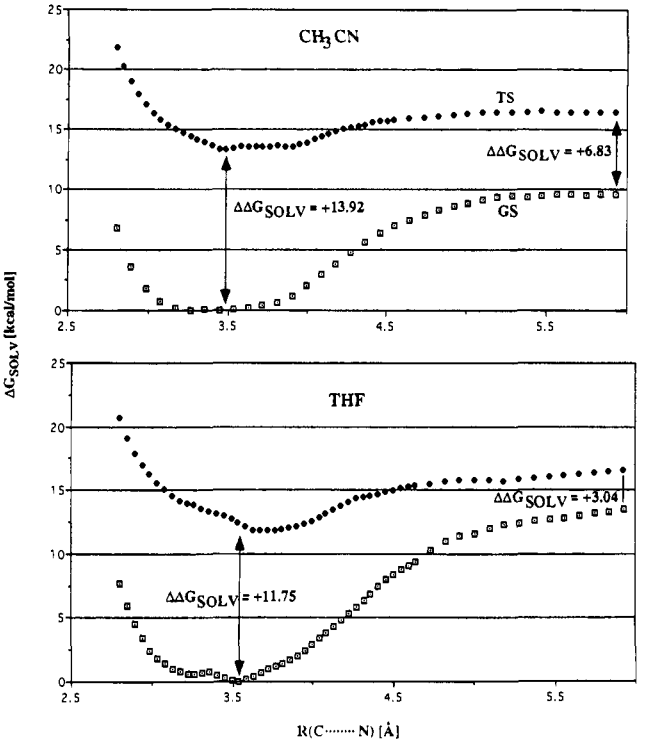

Figure 9. Free energy of solvation profile for the separation of benzisoxazole-3-carboxylate and tetramethylguanidinium ions in acetonitrile and tetrahydrofuran.

as the distance between carboxylate carbon and the NH_2 nitrogen atom. This distance was enlarged in increments of 0.046 Å up to a total distance of 5.928 Å, and the changes in free energy of solvation are calculated for each step.

The resulting free energy of solvation profile for the ground states is shown for acetonitrile and for tetrahydrofuran in Figure 9. For the benzisoxazole-3-carboxylate ground state, a steady increase in free energy of solvation is found until a plateau region is reached at an intermolecular distance of ca. 3.2 Å. This minimum corresponds to a loose ion pair and stretches from a distance of ca. 3.2 to 3.7 Å. Further separation results in a decrease of free solvation energy until the ions are ca. 5.2 Å apart. The free energy of solvation curve then flattens out considerably, especially in acetonitrile. The curve keeps going up slightly in THF up to the limit of ca. 6 Å. At this distance, the system can best be described as solvent-separated ion pairs with one layer of solvent molecules between the ions. The difference in solvation free energy between the minimum at ca. 3.5 Å and the final value at ca. 6 Å is larger in THF (+13.5 kcal/mol) than in acetonitrile (+9.6 kcal/mol). That is, the ground state ion pair is harder to separate in THF than in acetonitrile. The same trend can be observed for the transition state ion pairs. The minimum in the curve now extends from ca. 3.5 to 3.9 Å. The free energy necessary for separation of the ions is, however, much smaller than that for the ground state ion pairs, and the curves for both solvents are correspondingly flatter. The free energy of solvation required to separate the ion pair is larger in THF (+4.8 kcal/mol) than in acetonitrile (+3.1 kcal/mol). Including the extra energy required for the dissociation of the ion pairs for acetonitrile and THF into the difference in free energy of solvation between ground and transition states, and comparing these values with the values for water (where ion pairs are unlikely), one arrives at a dramatically altered picture (Table 4, BOSS $\Delta\Delta G_{solv}$, last column). The rates for acetonitrile and THF are now underestimated relative to water. As discussed before, this can likely be traced to the overestimation of Coulomb effects. The

inclusion of ion pairing effects improves, however, the calculation of the rate difference between THF and acetonitrile. The experimental difference in free energy of activation amounts to −0.3 kcal/mol. Without ion pairing, a value of −3.8 kcal/mol is obtained; that is, the reaction is calculated to occur much faster in THF than it actually is. Inclusion of ion pairing reduces this difference in free energy of activation to −1.5 kcal/mol. Even though the conclusion is not yet warranted by appropriate experimental data, ion pairing effects also seem to be substantial in acetonitrile.

The exploration of the free energy of solvation profile at much longer distances is desirable in order to exclude the possibility of favorable ion pairs separated by multiple layers of solvent molecules. To calculate free energy of solvation profiles up to an intermolecular distance of 25 Å, it would be necessary to choose a much larger solvent box, at least in one dimension, to avoid edge effects. Since the direct interactions between the ions are screened strongly by solvent molecules, the free energy differences at longer distances will also be significantly influenced by the interactions of the solvation shells of the ions with each other as well as the interaction of the solvation shell of one ion with the other ion. The cutoff for the solvent−solvent and solvent−solute interactions must therefore be adjusted to the larger intermolecular distances.

Conclusion

The ab initio calculations show that hydration of specific functional groups causes substantial shifts in transition state geometries along with changes in activation energy. The experimental isotope effect differences in solution and antibody are indicative of some change in the nature of the transition state. The solution simulations predict even greater solvent effects than are found experimentally. The results are attributed to possible problems in charge estimation or ion pairing effects.

Acknowledgment. We are grateful to the National Science Foundation for financial support of this research and the Office of Academic Computing at UCLA for computer time on the IBM ES9000/900 supercomputer and the RS6000 workstation cluster. Hendrik Zipse acknowledges support of the Deutsche Forschungsgemeinschaft and Göksin Apaydin acknowledges the Scientific and Technical Research Council of Turkey for a NATO fellowship. We thank Prof. William L. Jorgensen for the BOSS program and helpful advice.

Supporting Information Available: Listing of absolute energies for all stationary points (11 pages). This material is contained in many libraries on microfiche, immediately follows this article in the microfilm version of the journal, can be ordered from the ACS, and can be downloaded from the Internet; see any current masthead page for ordering information and Internet access instructions.

JA942130B